# Encapsulating Quantum Dots into Enveloped Virus in Living Cells for Tracking Virus Infection

**Yuan Zhang,[†,§] Xianliang Ke,[†,§] Zhenhua Zheng,[†] Cuiling Zhang,[‡] Zhenfeng Zhang,[†] Fuxian Zhang,[†] Qinxue Hu,[†] Zhike He,[‡] and Hanzhong Wang[†,*]**

[†]State Key Laboratory of Virology, Wuhan Institute of Virology, Chinese Academy of Sciences, Wuhan 430071, China and [‡]Key Laboratory of Analytical Chemistry for Biology and Medicine (Ministry of Education), College of Chemistry and Molecular Sciences, Wuhan University, Wuhan 430072, China. [§]These authors contributed equally to this work.

**ABSTRACT** Utilization of quantum dots (QDs) for single virus tracking has attracted growing interest. Through modification of viral surface proteins, viruses can be labeled with various functionalized QDs and used for tracking the routes of viral infections. However, incorporation of QDs on the viral surface may affect the efficiency of viral entry and alter virus–cell interactions. Here, we describe that QDs can be encapsulated into the capsid of vesicular stomatitis virus glycoprotein (VSV-G) pseudotyped lentivirus (PTLV) in living cells without modification of the viral surface. QDs conjugated with modified genomic RNAs (gRNAs), which contain a packaging signal (Psi) sequence for viral genome encapsulation, can be packaged into virions together with the gRNAs. QD-containing PTLV demonstrated similar entry efficiency as the wild-type PTLV. After infection, QD signals entered the Rab5+ endosome and then moved to the microtubule organizing center of the infected cells in a microtubule-dependent manner. Findings in this study are consistent with previously reported infection routes of VSV and VSV-G pseudotyped lentivirus, indicating that our established QD packaging approach can be used for enveloped virus labeling and tracking.

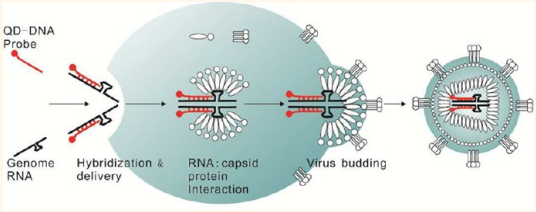


**KEYWORDS:** virus tracking · quantum dot · encapsulation · enveloped virus

Single virus tracking presents a powerful tool for exploring the mechanisms of viral infections. QDs, which have remarkable brightness and photostability, are excellent fluorescent probes for tracking various biological processes,[1−4] including long-term visualization of the movements of individual viral particles. Various functionalized QDs labeled on virus-like particles (VLPs), non-enveloped or enveloped viruses, combined with cell staining, have been used to reveal previously unobservable infection details and dynamic interactions between viruses and cellular components.[5−9]

In the application of QDs for single virus tracking, the most challenging problem is how to tag QDs to viral particles without affecting the viral entry routes. Several studies have demonstrated that QDs or other nanoparticles can be encapsulated into a viral capsid *in vitro* to form QD-containing VLP (VLP-QD)[9−11] or conjugated to the viral surface after virus production.[5−8,12−14] VLP-QD is generated by self-assembly of purified and concentrated major viral capsid proteins in appropriate conditions *in vitro*, but such an approach is not suitable for labeling enveloped viruses because viral envelopes are acquired from cell membranes when budding from host cells.[15] The most widely used approach to label enveloped viruses is to tag QDs to the viral surface through biotinylation,[6,7,14] modification with a clickable group,[16] or electrostatic attraction force after treatment.[12] However, most cellular receptor binding sites, which are essential for viral attachment and entry, are located on the viral surface, thus tagging QDs to viral surface proteins or modifying the viral surface for labeling could affect the efficiency of viral entry. In addition, QD labeling was found to affect the trafficking of various bioligands.[17−21] When QDs are tagged to the viral surface, the interaction between viruses and host cells could be artificially altered.[17−21] Furthermore, membrane fusion between the viral envelope and the cellular membrane could result in

* Address correspondence to wanghz@wh.iov.cn.

Received for review November 7, 2012 and accepted April 7, 2013.

**Published online April 08, 2013**
**10.1021/nn305189n**

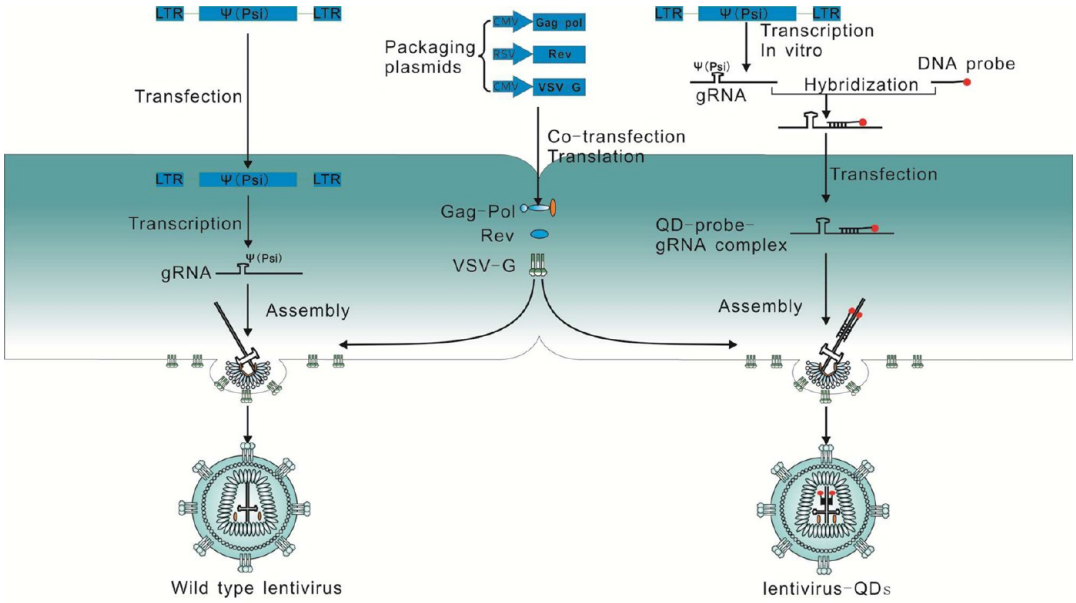


**Figure 1. Working principle of encapsulating SA-QDs into HIV-1-based lentivirus in living cells. In the HIV-1-based lentiviral system, the packaging plasmids express HIV-1 structure proteins Gag, Pol, and envelope protein VSV-G, and the transfer vectors generating gRNAs containing a packaging signal are co-transfected into packaging cells. gRNAs are encapsulated into the viral capsid through the interaction between Psi and Gag protein. Generated PTLVs acquire the envelope by budding from the infected cells (shown in the left part). When the transfer vectors are replaced with SA-QD-labeled gRNAs (shown in the right part), the QDs are encapsulated into the viral capsid together with the gRNAs to generate PTLV-QD. PTLV = pseudotyped lentivirus, LTR = long terminal repeat, Psi = packaging signal, gRNA = genomic RNA, SA-QD = QD625-streptavidin conjugate.**

disassociation of QDs with the viral capsid if QDs are tagged to the viral surface,[22−24] making it impossible to trace the late events of viral entry. In contrast, encapsulating QDs into enveloped viral capsids may be one option to tackle these problems.

The HIV-1-based lentiviral system is a safe and useful tool for studying enveloped viruses.[25,26] Through co-transfection of individual plasmids encoding HIV-1 structural proteins, enzymes, and genome RNAs, replication-deficient viruses with authentic viral structures can be generated (as illustrated in Figure 1, left). By replacing the envelope protein-expressing plasmid, different glycoprotein pseudotyped lentiviruses (PTLVs) can be produced.[25,26] Given that the entry pathways of enveloped viruses are directed by viral envelope glycoproteins, this system can be used for studying the entry of different enveloped viruses.

Here we described an approach for encapsulating QDs inside the core of VSV glycoprotein (VSV-G) pseudotyped HIV-1-based lentivirus during virus assembly in living cells. In the life cycle of HIV-1, the interaction between Gag protein and packaging signal (Psi) sequence on 5′LTR of gRNA is critical for genome packaging and virus assembly.[27−29] Capsid protein of red clover necrotic mosaic virus (RCNMV), a non-enveloped plant virus which employs a similar mechanism to pack its two genomic ssRNAs, has been shown to package nanoparticles (NP) conjugated with its genomic RNA to form NP-containing VLPs.[10,30] We adopt a similar packaging strategy to encapsulate QDs into VSV-G pseudotyped HIV-1-based lentivirus in living cells instead of *in vitro*. Modified genomic RNAs (gRNAs) of HIV-1-based lentivirus hybridized with QD-DNA probes are delivered into packaging cells transfected with plasmids which express structure and envelope proteins. PTLV with QD labeling on the gRNAs can be obtained during virus production in living cells (as illustrated in Figure1, right). Using this approach, no surface modification of the virus is required and the entry route and entry efficiency are not affected. Taken together, we have established a QD-labeling approach by using VSV-G PTLV as a model, and this technology may be applicable for investigating the infection routes directed by envelope proteins of other viruses.

## RESULTS AND DISCUSSION

QD-based probes and beacons delivered into cells have been used to image the behaviors of cellular mRNA[31] or viral components after infection.[31,32] In the current study, to produce QD-labeled PTLV, a QD-DNA probe−gRNA complex was synthesized *in vitro*. Briefly, a QD-DNA probe was formed by interaction between a QD−streptavidin conjugate (SA-QDs) and biotinylated DNA probes targeting genomic RNA (gRNA) of HIV-1 lentivirus. The QD probe was then hybridized with gRNAs produced by transcription *in vitro* to form the QD-DNA probe−gRNA complexs. Interestingly, we found that the length of the gRNA greatly influenced the packaging efficiency of the complex (data not shown). While the mechanism is unclear, a modified gRNA with

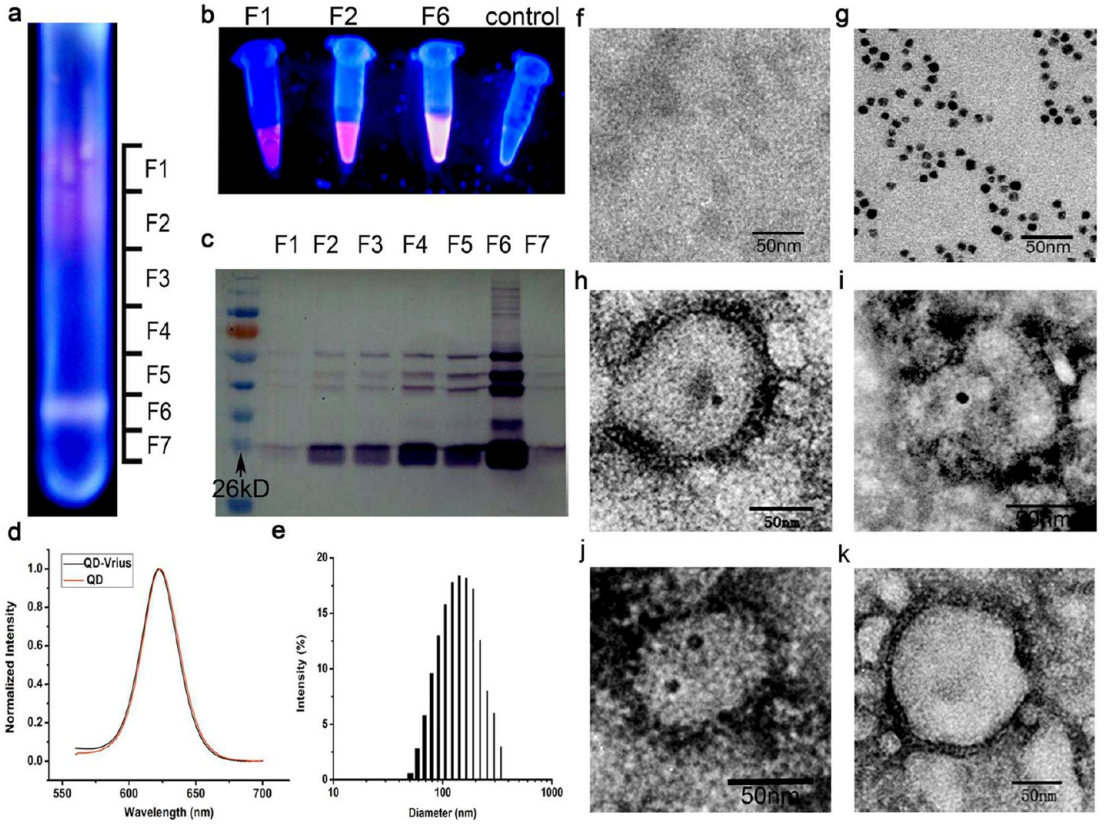


**Figure 2. Purification and characterization of PTLV-QD. (a) Image of the SDGC tube after the separation of PTLV-QD under a UV lamp. (b) Image of fluorescent fractions F1, F2, and F6 under a UV lamp after further purification to remove sucrose. (c) Content of p24 in F1−F7 analyzed by Western bloting. (d) Fluorescence spectra of PTLV-QD compared with QDs. (e) DLS distribution *versus* $D_h$ of PTLV-QD. (f−k) TEM images of negative staining reagent (f), SA-QD (g), PTLV encapsulating one QD particle (h,i), two QD particles (j), and wild-type PTLV (k). All samples were stained for 10 s (scale bar: 50 nm).**

deleted sequence that is not essential for virus assembly and genome packaging was used to generate the QD-DNA probe−gRNA complex in order to achieve maximum efficiency. The complex was then delivered into HEK293T transfected with structure protein and envelope protein-expressing plasmids. This procedure mimics the packaging behaviors of wild-type HIV-1.

Sucrose density gradient centrifugation (SDGC) was employed to purify PTLV-QD from the supernatants of packaging cells containing PTLV-QD, redundant proteins, QDs, and QD-DNA probe−gRNA complexes as reported.[33] After SDGC, seven fractions were divided and collected from top to bottom in the SDGC tube (Figure 2a). F1, F2, and F6 showed fluorescence under an ultraviolet lamp. Each fraction was further purified to remove redundant sucrose. The final products were collected in a tube and examined under an ultraviolet lamp (Figure 2b). The content of HIV-1 structural protein p24 in each fraction was examined by Western blotting (Figure 2c). F6 contained the majority of p24, and it was also the major fluorescent band. Therefore, this fraction was collected for subsequent characterization.

To confirm that F6 (see above) contained QD-labeled PTLV rather than a mixture of PTLV and QDs, an immunofluorescence test was performed. The virus solution was overlaid onto coverslips (Figure 3b) or added to HeLa cells to allow virus attachment (Figure 3a) and then immunostained with an antibody against HIV capsid protein (p24). About 75−80% of p24 colocalized with QD signals, while most of the QDs colocalized with p24, suggesting that the produced PTLVs were labeled with QDs and all of the QD signals represented PTLV particles. There were 20−25% of unlabeled PTLVs (green) after purification, which might be virus-like particles (VLPs) without genome formed by Gag and VSV-G as reported[34] or PTLV containing gRNA without QDs.

PTLV-QDs were also characterized by TEM (Figure 2f−k), while negative-staining reagent (Figure 2f), SA-QDs (Figure 2g), and wild-type PTLV (Figure 2k) were used as controls. After negative staining, pure SA-QDs showed a dark electron dense core with a size of ~10 nm (Figure 2g). In the PTLV-QD sample, a dark electron dense core with the same size was seen inside of the virion (Figure 2h−j). Most PTLV-QDs showed similar morphology as wild-type PTLV (Figure 2k), indicating that this labeling approach did not interfere with viral morphogenesis. These results also confirmed the colocalization results of p24-FITC and QDs, indicating that QDs were encapsulated into PTLV rather than

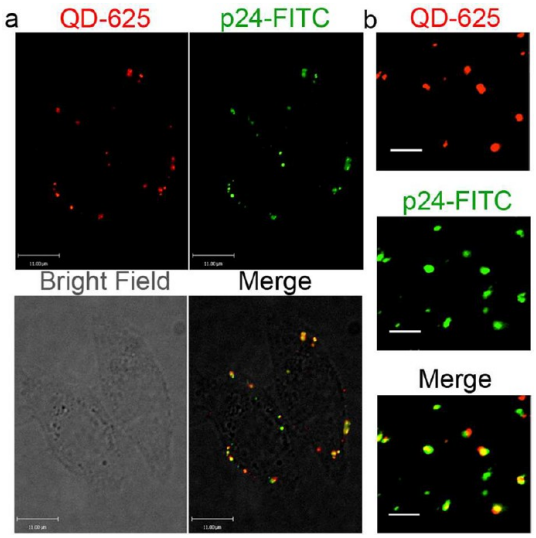


**Figure 3. Immunofluoresence assay. (a,b) Immunofluorescence assay using anti-p24 antibody as primary antibody and FITC-conjugated goat anti-rabbit IgG as second antibody against PTLV-QD attached to HeLa cells (a) (scale bar: 11 $\mu$m) or overlaid on polylysine-coated coverslips (b) (scale bar: 2 $\mu$m).**

nonspecifically attached to viral surface. There were some virus particles containing no SA-QD in the PTLV-QD sample (not shown), which were likely to be the incomplete packaging of QDs. Statistical analysis of the PTLV-QD particles observed through TEM revealed that 34.07% (31/91) of PTLV-QD encapsulated one QD particle and 65.93% (60/91) of PTLV-QD encapsulated two QD particles. This was likely because PTLV packages double-stranded gRNAs but not all of the gRNAs were labeled with SA-QDs successfully.

Fluorescence spectra (Figure 2d) and dynamic light scattering (DLS) (Figure 2e) tests were performed to further characterize PTLV-QD particles. Compared with SA-QD alone, the spectrum of PTLV-QD had a blue shift around 1 nm (Figure 2d). The phenomenon may be attributed to the change of electronic properties of QDs caused by DNA coupled on the surface. The distribution of hydrodynamic diameter ($D_h$) measured by dynamic light scattering (DLS) for PTLV-QD in aqueous solution was characterized (Figure 2e). The average $D_h$ is 159.4 nm, which is a little larger than the actual diameter (100−140 nm shown in the TEM analysis), due to the influence of the counterion cloud on particle mobility.

To test whether the PTLV-QD particles could enter cells, HeLa cells were incubated with SA-QDs and PTLV-QD to allow attachment and entry. Compared with SA-QD, PTLV-QD exhibited a totally different fate. PTLV-QD attached and entered HeLa cells with high efficiency and was completely internalized into cells (Figure 4a), and all of the cells appeared to uptake PTLV-QD. In contrast, SA-QD showed very little uptake by cells even after 8 h incubation (Figure 4b). To further confirm that the QD signals observed in the PTLV-QD-incubated cells were indeed due to virus infection, a viral neutralization assay was performed. An antibody specifically against VSV-G was used to neutralize the envelope protein of the PTLV-QD to block virus attachment to cellular receptors. It was found that, once the virus was neutralized by the VSV-G antibody, PTLV-QD particles were barely attached to the cell surface and no uptake was observed by visualizing QD signals (Figure 4c), further reinforcing the idea that the internalization of QDs was directed by VSV-G PTLV.

To determine whether our approach affects the efficiency of virus entry, purified PTLV-QD and wild-type PTLV were titered by real-time PCR. The titer of PTLV-QD was 1/82.59 of the wild-type PTLV (Figure 4d), suggesting that replacement of the gRNA-generating plasmid with transfected gRNA produced *in vitro* reduces PTLV production. These two viruses with equal numbers of RNA copies were used to infect HEK293T cells. Total RNA was extracted from infected cells 2 h postinfection and subjected to real-time PCR to determine intracellular viral RNA copy number. The intracellular RNA copy number of PTLV-QD was a little higher than that of the wild-type PTLV (Figure 4d), indicating that there was no decrease of viral entry efficiency after QD labeling.

Having proven that PTLV-QD can enter mammalian cells, we next tested whether this labeling approach could be used to monitor virus transport in sensitive cells. Most enveloped viruses, including VSV[35,36] and VSV-G PTLV,[37] enter cells *via* endocytosis and require the fusion of the viral envelope with the endosome membrane. To investigate the movement of PTLV to the endosomes, HeLa cells were transfected with Rab5-EGFP to mark the early endosomes[6] and then incubated with PTLV-QD for infection. PTLV-QD infected cells were fixed and subjected to confocal analysis at different time points. Ten minutes postinfection, PTLV-QD (red) showed no colocalization with early endosomes marker Rab5 (green). At 30 min postinfection, QDs showed significant colocalization with early endosomes (Figure 5a), suggesting that PTLV-QD particles were transported to Rab5+ endosomes after endocytosis. Real-time tracking of the transport of single PTLV-QD to early endosomes was also performed, and representative images are shown in Figure 5b. At 20 min postinfection, PTLV-QD particles (red) were close to the Rab5+ organelle (green). After internalization initialized at 21 min, PTLV-QD remained within the Rab5+ endosome (yellow) for an extended period of time (22−27 min). Thus, a clear process of PTLV-QD internalization was monitored, which was consistent with that reported by previous virus tracking studies.[6]

To further elucidate infection details, an experiment focusing on the movement to a microtubule organizing center (MTOC) was performed. After internalization, many viruses need to be transported to the MTOC compartment, where their genetic material is released

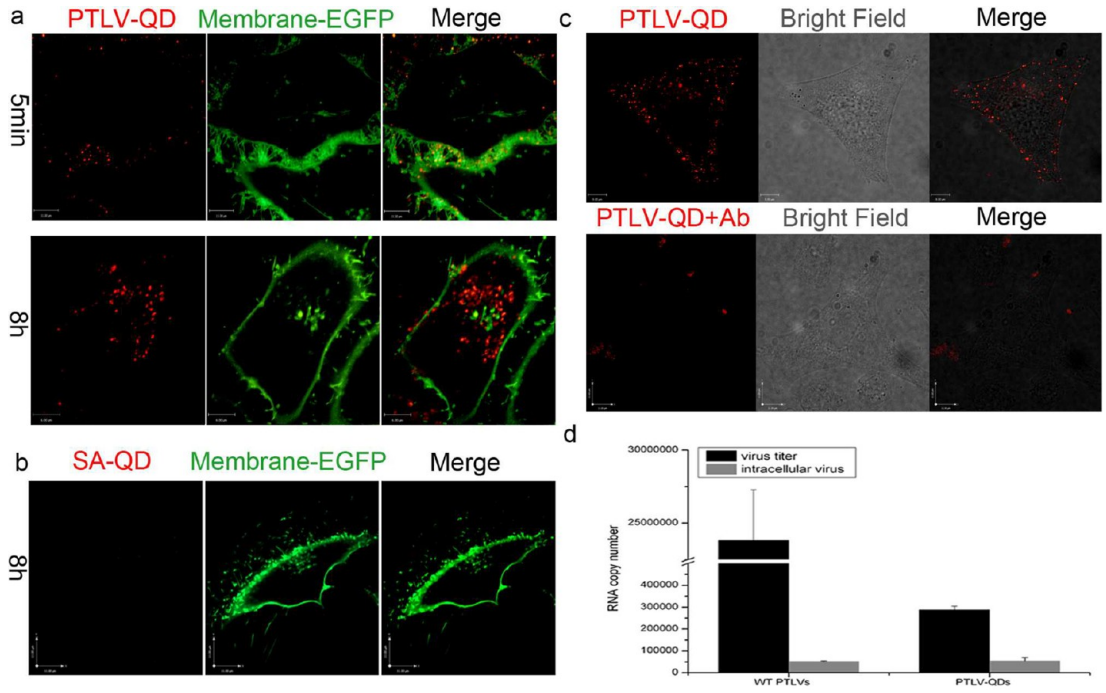


**Figure 4. Infection of cells by PTLV-QD. (a,b) Comparison of PTLV-QD and SA-QD infected HeLa cells. HeLa cells were transfected with membrane EGFP plasmid 36 h before infection. (a) PTLV-QD still attached to HeLa cell membranes 5 min after infection (scale bar: 11 $\mu$m) and was totally uptaken by cells 8 h after infection (scale bar: 6 $\mu$m). (b) SA-QD alone showed no uptake by HeLa cells after 8 h incubation (scale bar: 11 $\mu$m). (c) Images of HeLa cells infected with PTLV-QD or PTLV-QD neutralized by VSV-G antibody for 30 min (scale bar: 11 $\mu$m). (d) Cell entry efficiency of wild-type PTLV and PTLV-QD. Titers of PTLV-QD compared with PTLV tested by real-time PCR are shown as the black column. PTLV-QD and PTLV containing equal copies of RNA were used to infect HEK293T cells. Intracellular viral RNA copy numbers, representing the entry efficiency of PTLV, are shown as the gray column.**

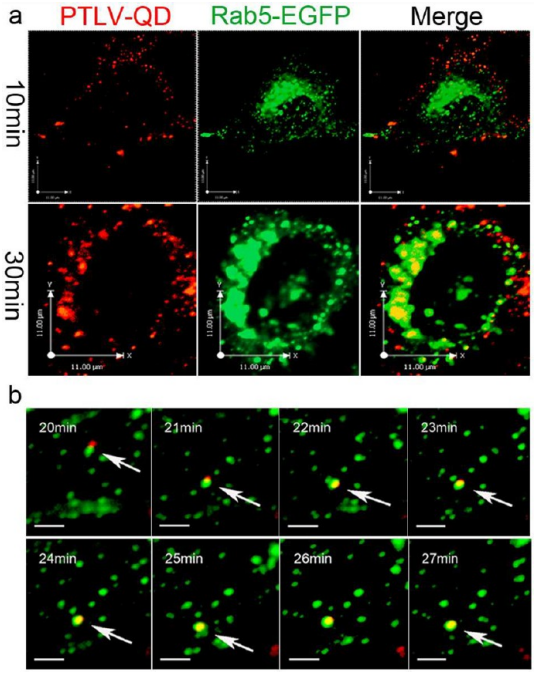


**Figure 5. Tracking the movement of PTLV-QD to Rab5+ endosomes. (a) HeLa cells were incubated with PTLV-QD for 10 or 30 min after transfected with Rab5-EGFP (scale bar: 11 $\mu$m). (b) Real-time tracking of PTLV-QD transported to early endosomes (Rab5+). PTLV-QD was incubated with HeLa cells, and then the real-time images were recorded at indicated time points (scale bar: 2 $\mu$m).**

to the cytosol or delivered into the nucleus to start replication.[38] Previous study has proven that the transport of VSV to MTOC is facilitated by microtubules.[37] To investigate the role of microtubules in VSV-G PTLV entry, PTLV-QD was used to infect HeLa cells. HeLa cells were transfected with a microtubule-EGFP plasmid to mark the microtubule and fixed for confocal imaging at indicated time points after infection (10, 40, and 100 min). At 10 min, no PTLV (red) colocalized with GFP-tagged microtubules. PTLV-QD movement on microtubules was observed at 40 min postinfection, and about 90% of PTLV-QD particles in cells converged at MTOC 100 min postinfection (Figure 6a). Single virus trajectories on microtubules were also recorded, and representative images were shown in Figure 6f. To confirm whether the movement toward MTOC was microtubule-dependent, nocodazole, a drug to disturb microtubules, was used to treat HeLa cells before infection. The trajectory and velocity of the single virus particle were analyzed (Figure 6b–e). In untreated HeLa cells, PTLV-QD moved from the cell periphery to the cytoplasm with a long trajectory (Figure 6b) and showed an active movement pattern (Figure 6c). PTLV experienced an intermittent moving stage (0–200 s, average speed 0.0105 $\mu$m/s) and then traveled rapidly toward the cytoplasm (200–400 s, average speed 0.0705 $\mu$m/s) with a max instantaneous speed

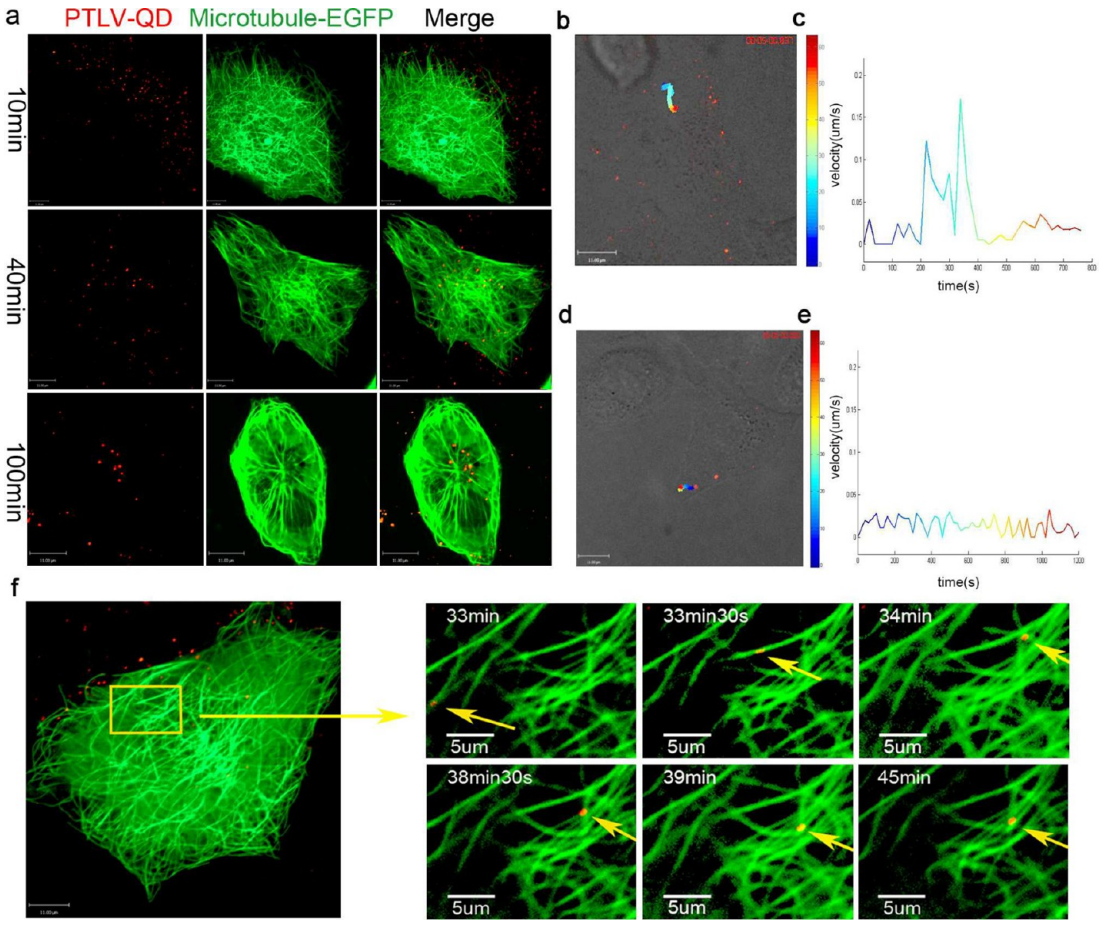


**Figure 6. Tracking the microtubule-dependent entry pathway of PTLV-QD. (a) PTLV-QD was incubated with the cells for 10, 40, and 100 min (scale bar: 11 $\mu$m). HeLa cells were transfected with the EGFP-microtubule plasmid 36 h before PTLV-QD infection. (b,c) Trajectory and the instantaneous speed of individual PTLV-QD in living cells (scale bar: 11 $\mu$m). (d,e) Trajectory and the instantaneous speed of individual PTLV-QD in living cells after treatment with 70 $\mu$M nocodazole (scale bar: 11 $\mu$m). (f) Real-time tracking of PTLV-QD transported along the microtubule to the perinuclear region. PTLV-QD was incubated with the cells for 25 min, and then the real-time images were recorded (scale bar: 5 $\mu$m).**

of 0.1713 $\mu$m/s. Finally, PTLV particles moved slowly and confinedly (400−760 s, average speed 0.0164 $\mu$m/s) somewhere in the cytoplasm (Figure 6c). In contrast, in nocodazole-pretreated HeLa cells, PTLV moved around the cell membrane with very short trajectory (Figure 6d), and the instantaneous speed was low (average speed 0.0141 $\mu$m/s), showing tiny fluctuations in the whole tracking period (Figure 6e). These two different transport modes indicated that nocodazole can strongly inhibit virus traffic during infection. Our results are in agreement with previously reported infection mechanisms of other enveloped viruses such as HIV, reovirus, influenza, and HSV.[7,39−42] In addition, we observed that PTLV-QD moved along the microtubule (Figure 6f), providing visible details for microtubule-dependent transport of VSV infection.[37]

Nanomaterials, including QDs and gold nanoparticles, were previously shown to be packaged inside the VLPs of non-enveloped viruses red clover necrotic mosaic virus (RCNMV)[10,30] and SV40.[9,43,44] In those reports, a specific RNA−protein interaction *in vitro* that initiates genomic RNA packaging was used to achieve controlled encapsidation of Au, $CoFe_2O_4$, and CdSe nanoparticles into RCNMV VLPs.[10,30] Self-assembly of SV40 VP1 protein *in vitro* could also achieve high efficiency of nanoparticle packaging.[9,43,44] Although these studies provide useful information for virus labeling, such an *in vitro* packaging approach is not practical for labeling enveloped viruses because enveloped viruses have envelopes that consist of phospholipids and proteins, which are usually derived from host cell membranes.

Wang *et al.* provided the first biocompatible approach for enveloped virus labeling by expressing a biotin acceptor peptide on a viral membrane followed by site-specific labeling with streptavidin-conjugated QDs.[6] Other functional peptide biotin-based QD labeling and chemical coupling or click-based QD-labeling methods have also been developed for tagging the viral envelope with QDs.[7,8,12,14,16,45,46] These inspiring improvements of labeling approaches have been used to reveal the infection details of IHNV, H9N2, PTLV, retrovirus, Sindbis virus, baculovirus, and PrV.[7,8,12,14,16,45,46] Given that the viral envelope plays an essential role in cell entry,[23] modification of the viral membrane for

labeling could decrease viral entry efficiency. Indeed, labeling QDs on the viral surface of IHNV[8] and PrV[14] resulted in an slightly impaired infectivity, which may be caused by an influenced virus entering process. Our study demonstrated that the modified HIV-1 gRNAs containing 5′LTR and Psi were able to smuggle QDs into the core structures of PTLV during virus assembly. Our procedure of packaging QDs inside the capsids of virus progenies in living cells does not require biological or chemical modification of the viral surface and causes no change of viral morphology, thus assuring the viral entry efficiency. This was confirmed by the quantitative analysis of viral RNA copies in infected cells.

Although QDs have been used for probing viral entry, it remains controversial as to whether QD labeling affects the uptake routes of biomolecules by cells. Most QD-labeled ligands showed trafficking characteristics similar to that of unlabeled ligands. However, examples of altered behaviors of bioligands after QD labeling still exist.[17] QDs can reduce or increase the normal endosome-to-Golgi transport efficiency of several toxin ligands,[21] and in some cases, the innate uptake is inhibited. Commercial QDs, typically 20−30 nm in size, can hinder AMPA (α-amino-3-hydroxy-5-methyl-4-isoxazolepropionate)receptors from entry into neuronal membrane synapses.[18] For instance, a slower membrane fusion of glutamate receptors was observed when QDs rather than traditional fluorescent dyes were used.[19] When QD-labeled antibodies were used to track single potassium channel proteins, the type of diffusion was significantly changed.[20] Additionally, multivalency of QDs may result in cross-linking of labeled proteins and the activation of signal pathways, thus interfering with the imaging results. It was reported that these anomalous results were caused by potential interactions between QDs and cellular components.[17,18] In our study, QDs in virions are physically separated from cellular environments by the viral capsid and the envelope. In such conditions, QDs are unlikely to interact with cellular components and, therefore, avoid the alteration of viral movements. The movement of PTLV-QD in infected cells observed in our study is not in conflict with previous studies, indicating that the virus transport route was not influenced by this QD-encapsulating strategy.

Although further improvement may be needed, our established QD-packaging approach is potentially useful in tracking infection events postmembrane fusion. Membrane fusion is crucial for enveloped virus penetration and the release of genetic material.[22−24] Fusion directed by viral glycoprotein can happen at the plasma membrane at neutral pH or in the endosomal membrane under a lower pH.[23] Using conventional methods, fluorescent materials labeled on the viral envelope usually dissociate from the viral core after virus−cell membrane fusion, making it impossible to track the journey of the cores of enveloped viruses from entry to capsid disassembly.[47] For example, single virus trafficking through labeling lipophilic dye DiD on the membrane of HIV core-based pseudoviruses was used to track the membrane fusion, but DiD disappeared upon membrane fusion.[48] Our strategy of encapsulating QDs inside virus cores makes it possible to elucidate the trafficking of the virus capsid before disassembly.

Despite the favorable characteristics of our approach, further improvement may be needed. For instance, because SA-QDs are membrane-impermeable and can be trapped in the endosomes,[49] the yield of effective labeled viruses is affected. Using cell-penetrating QDs that could easily release from organels is one alternative in future study to increase the packaging efficiency. In addition, we found that QD-DNA probe−gRNA complexes prepared using short gRNAs enhanced the yield of PTLV-QD, in which the sequences that are not essential for gRNA encapsulation were deleted, although the deletion slightly impaired some functions of PTLV, such as protein expression and reverse transcription. Nevertheless, at the current stage, our packaging strategy has been proven to be able to produce enough viruses for virus tracking experiments. Further improvement of our method may render it useful in illuminating the motion of viral capsids and in tracking the postfusion events of labeled viruses.

## CONCLUSION

In conclusion, we have designed and evaluated a method which could encapsulate QDs into an enveloped virus in living cells. This method may facilitate the application of nanoparticles in biological imaging, including the infection events directed by different viral envelopes in late infection period.

## METHODS

**Plasmid Construction.** HIV-1-based lentiviral vector plentilox3.7 was purchased from Addgene. To construct the modified gRNA transcription template pT-ePsi, 835−1586 bp of plentilox3.7, containing HIV-1 5′LTR and packaging signal which are essential for virus assembly and genome packaging, was amplified by PCR using primers LP-F(ACATGCATGCGGGTCTCTCTGGTTAGACCA) and LP-R(CCGGAATTCTCACTTCTCCAATTGTCCCT). PCR product was subsequently cloned into pGEM-T easy vector under the T7 promotor.

**Preparation of QD-DNA Probe−gRNA Complexes.** QD625-streptavidin conjugate was purchased from Invitrogen. DNA probe (CTGATCTTCAGACCTGGAGGAGGAGATATGAGGGACAATTGGAGAAGTGA) biotinylated at the 5′ end was synthesized by Invitrogen. The probe and QD625-streptavidin conjugate were then combined in PBS (pH 7.4) at a ratio of 4:1 and incubated at 37 °C for 3 h to produce a QD-based DNA probe through specific interaction between streptavidin and biotin. To produce genomic RNAs, plasmid pT-ePsi was linearized using *Eco*RI digestion, purified using Cycle Pure kit (Omega), and then subjected to *in vitro* transcription using RiboMAX large-scale RNA production

systems (Promega) according to the manufacturer's protocol. The resulting RNAs were incubated with the QD-DNA probe at a ratio of 1:1 to form QD-DNA probe−gRNA complexes by complementary base pairing.

**Production of PTLV-QD.** 293T cells were maintained in a 37 °C, 5% $CO_2$ environment in Dulbecco's modified Eagle medium (DMEM) supplemented with 10% FBS (Gibico). Eighteen hours before transfection, 293T cells were seeded in 100 mm dishes. Packaging vectors pLP1 and pLP2, which express the HIV structure proteins Gag and Pol, respectively, and vector pLP/VSVG expressing the VSV glycoprotein were co-transfected into 293T cells using 1 $\mu$g/$\mu$L polyethylenimine (PEI) (Sigma). Medium was changed 5 h post-transfection. Subsequently, the QD-DNA probe-ePsi RNA complexes were delivered into 293T cells by a second transfection using lipofectamine 2000 (Invitrogen).

**Virus Purification.** Cell culture supernatants were harvested every 24 h after QD-probe-RNA complex transfection and supplemented with fresh medium until day 6. To remove cell debris, the collected supernatants were subjected to centrifugation at 4000*g* for 30 min at 4 °C, filtered through a 0.45 $\mu$m filter (Milipore), and then concentrated by centrifugation at 23 000 rpm for 1.5 h at 4 °C. The pellet was then layered on 20−60% sucrose density gradient followed by centrifugation at 35 000 rpm, 4 °C for 3 h in an SW40 Ti rotor (Beckman). Fractions containing QDs were collected under UV excitation and centrifugated at 23 000 rpm for 1.5 h at 4 °C to remove sucrose. Virus was resuspended in PBS (pH 7.4) for further experiments.

**Transmission Electron Microscopy.** For TEM examination, a carbon-coated copper grid was laid on the purified samples (10 $\mu$L) for 5 min. After removal of the redundant liquid using filter papers, the prepared samples were negatively stained with 1% phosphotungstate (10 $\mu$L) for 10 s and subsequently examined under a Hitachi H7000 electron microscope.

**Viral Neutralization.** For the neutralization experiment, 5 $\mu$g/$\mu$L antibody against VSV-G protein was added to the purified PTLV and incubated at 37 °C for 3 h. The neutralized virus or unneutralized virus was then used to infect HeLa cells and examined using a fluorescence microscope.

**Real-Time PCR.** Viral and total cellular RNAs were extracted using Trizol reagent (Invitrogen), retro-transcribed to cDNAs using the primer HIV antisense (TCGCGATCTAATTCTCCC), and then subjected to real-time PCR analysis on an Applied Biosystems StepOnePlus real-time PCR system using the primer HIV sense (CGAACAGGGACTTGAAAG), HIV antisense (TCGCGATCTAATTCTCCC), and a specific TaqMan probe (FAM-CGCTTAATACTGACGCTCTCGC-TAMRA).

**Fluorescence Microscopy.** For the immunofluorescence test, QDs, PTLV-QD, or PTLV was overlaid on polylysine-coated coverslips for 60 min at 37 °C or incubated with HeLa cells preseeded in 15 mm dishes (NEST Biotechnology) for 30 min at 4 °C, then shifted to 37 °C for 10 min incubation. Then coverslips or cells were rinsed, fixed with 4% formaldehyde, permeabilized with 2% Triton-X100, and immunostained with anti-p24 monoclonal antibody and FITC-labeled secondary antibody. Confocal laser scanning microscopy was performed on a PerkinElmer UltraView VOX system using a Nikon Ti microscope with 60× objectives.

**Virus Tracking.** For the viral tracking studies, subcellular structures were labeled through transfection of HeLa cells with individual plasmids encoding either GFP membrane, GFP-Rab5, or GFP-microtubule. Thirty-six hours post-transfection, PTLV-QD or PTLV was incubated with cells for 30 min at 4 °C to synchronize infection. The cells were shifted to 37 °C for infection and subjected to real-time trafficking at different time points.

**Drug Inhibition Assay.** In the microtubule drug inhibition assay, PTLV-QD was used to infect HeLa cells pretreated or untreated with 70 $\mu$M nocodazole at 18 °C for 1 h. Real-time tracking of virus infection routes was taken very 20 s between 0 and 20 min following infection. Image-Pro Plus and MATLAB were used to analyze the trajectory and velocity of single virus particle.

**Dynamic Light Scattering.** Dynamic light scattering (DLS) measurements were performed on the Zetasizer instrument ZEN3600 (Malvern, UK) with a 173° back-scattering angle and He−Ne laser ($\lambda$ = 633 nm). QD-encapsulated PTLV was filtered with a 0.45 $\mu$m nitrocellulose filter to remove any interfering dust particles.

**Fluorescence Spectra.** Fluorescence spectra of QDs and QD-encapsulated PTLV was recorded on a Shimadzu RF-5301 spectrofluorometer.

*Conflict of Interest:* The authors declare no competing financial interest.

*Acknowledgment.* This work is supported by the National Key Scientific Program-Nanoscience and Nanotechnology (2011CB933600) and the National Basic Research Program of China (2010CB530100).

## REFERENCES AND NOTES

1. Smith, A. M.; Duan, H.; Mohs, A. M.; Nie, S. Bioconjugated Quantum Dots for *In Vivo* Molecular and Cellular Imaging. *Adv. Drug Delivery Rev.* **2008**, *60*, 1226–1240.
2. Medintz, I. L.; Uyeda, H. T.; Goldman, E. R.; Mattoussi, H. Quantum Dot Bioconjugates for Imaging, Labelling and Sensing. *Nat. Mater.* **2005**, *4*, 435–446.
3. Mattoussi, H.; Palui, G.; Na, H. B. Luminescent Quantum Dots as Platforms for Probing *In Vitro* and *In Vivo* Biological Processes. *Adv. Drug Delivery Rev.* **2012**, *64*, 138–166.
4. Jin, Z.; Hildebrandt, N. Semiconductor Quantum Dots for *In Vitro* Diagnostics and Cellular Imaging. *Trends Biotechnol.* **2012**, *30*, 394–403.
5. Joo, K. I.; Fang, Y.; Liu, Y.; Xiao, L.; Gu, Z.; Tai, A.; Lee, C. L.; Tang, Y.; Wang, P. Enhanced Real-Time Monitoring of Adeno-Associated Virus Trafficking by Virus−Quantum Dot Conjugates. *ACS Nano* **2011**, *5*, 3523–3535.
6. Joo, K. I.; Lei, Y.; Lee, C. L.; Lo, J.; Xie, J.; Hamm-Alvarez, S. F.; Wang, P. Site-Specific Labeling of Enveloped Viruses with Quantum Dots for Single Virus Tracking. *ACS Nano* **2008**, *2*, 1553–1562.
7. Liu, S. L.; Zhang, Z. L.; Tian, Z. Q.; Zhao, H. S.; Liu, H.; Sun, E. Z.; Xiao, G. F.; Zhang, W.; Wang, H. Z.; Pang, D. W. Effectively and Efficiently Dissecting the Infection of Influenza Virus by Quantum-Dot-Based Single-Particle Tracking. *ACS Nano* **2012**, *6*, 141–150.
8. Liu, H.; Liu, Y.; Liu, S.; Pang, D. W.; Xiao, G. Clathrin-Mediated Endocytosis in Living Host Cells Visualized through Quantum Dot Labeling of Infectious Hematopoietic Necrosis Virus. *J. Virol.* **2011**, *85*, 6252–6262.
9. Li, F.; Zhang, Z. P.; Peng, J.; Cui, Z. Q.; Pang, D. W.; Li, K.; Wei, H. P.; Zhou, Y. F.; Wen, J. K.; Zhang, X. E. Imaging Viral Behavior in Mammalian Cells with Self-Assembled Capsid-Quantum-Dot Hybrid Particles. *Small* **2009**, *5*, 718–726.
10. Loo, L.; Guenther, R. H.; Lommel, S. A.; Franzen, S. Encapsidation of Nanoparticles by Red Clover Necrotic Mosaic Virus. *J. Am. Chem. Soc.* **2007**, *129*, 11111–11117.
11. Dixit, S. K.; Goicochea, N. L.; Daniel, M. C.; Murali, A.; Bronstein, L.; De, M.; Stein, B.; Rotello, V. M.; Kao, C. C.; Dragnea, B. Quantum Dot Encapsulation in Viral Capsids. *Nano Lett.* **2006**, *6*, 1993–1999.
12. Chen, Y. H.; Wang, C. H.; Chang, C. W.; Peng, C. A. *In Situ* Formation of Viruses Tagged with Quantum Dots. *Integr. Biol.* **2010**, *2*, 258–264.
13. Cui, Z. Q.; Ren, Q.; Wei, H. P.; Chen, Z.; Deng, J. Y.; Zhang, Z. P.; Zhang, X. E. Quantum Dot−Aptamer Nanoprobes for Recognizing and Labeling Influenza a Virus Particles. *Nanoscale* **2011**, *3*, 2454–2457.
14. Huang, B. H.; Lin, Y.; Zhang, Z. L.; Zhuan, F.; Liu, A. A.; Xie, M.; Tian, Z. Q.; Zhang, Z.; Wang, H.; Pang, D. W. Surface Labeling of Enveloped Viruses Assisted by Host Cells. *ACS Chem. Biol.* **2012**, *7*, 683–688.
15. Cadd, T. L.; Skoging, U.; Liljestrom, P. Budding of Enveloped Viruses from the Plasma Membrane. *Bioessays* **1997**, *19*, 993–1000.
16. Zhang, P.; Liu, S.; Gao, D.; Hu, D.; Gong, P.; Sheng, Z.; Deng, J.; Ma, Y.; Cai, L. Click-Functionalized Compact Quantum Dots Protected by Multidentate-Imidazole Ligands: Conjugation-Ready Nanotags for Living-Virus Labeling and Imaging. *J. Am. Chem. Soc.* **2012**, *134*, 8388–8391.

17. Pinaud, F.; Clarke, S.; Sittner, A.; Dahan, M. Probing Cellular Events, One Quantum Dot at a Time. *Nat. Methods* **2010**, *7*, 275–285.
18. Howarth, M.; Liu, W.; Puthenveetil, S.; Zheng, Y.; Marshall, L. F.; Schmidt, M. M.; Wittrup, K. D.; Bawendi, M. G.; Ting, A. Y. Monovalent, Reduced-Size Quantum Dots for Imaging Receptors on Living Cells. *Nat. Methods* **2008**, *5*, 397–399.
19. Groc, L.; Lafourcade, M.; Heine, M.; Renner, M.; Racine, V.; Sibarita, J. B.; Lounis, B.; Choquet, D.; Cognet, L. Surface Trafficking of Neurotransmitter Receptor: Comparison between Single-Molecule/Quantum Dot Strategies. *J. Neurosci.* **2007**, *27*, 12433–12437.
20. Nechyporuk-Zloy, V.; Dieterich, P.; Oberleithner, H.; Stock, C.; Schwab, A. Dynamics of Single Potassium Channel Proteins in the Plasma Membrane of Migrating Cells. *Am. J. Physiol.* **2008**, *294*, 1096–1102.
21. Tekle, C.; Deurs, B.; Sandvig, K.; Iversen, T. G. Cellular Trafficking of Quantum Dot-Ligand Bioconjugates and Their Induction of Changes in Normal Routing of Unconjugated Ligands. *Nano Lett.* **2008**, *8*, 1858–1865.
22. Marsh, M.; Helenius, A. Virus Entry: Open Sesame. *Cell* **2006**, *124*, 729–740.
23. Harrison, S. C. Viral Membrane Fusion. *Nat. Struct. Mol. Biol.* **2008**, *15*, 690–698.
24. White, J. M.; Delos, S. E.; Brecher, M.; Schornberg, K. Structures and Mechanisms of Viral Membrane Fusion Proteins: Multiple Variations on a Common Theme. *Crit. Rev. Biochem. Mol. Biol.* **2008**, *43*, 189–219.
25. Funke, S.; Maisner, A.; Muhlebach, M. D.; Koehl, U.; Grez, M.; Cattaneo, R.; Cichutek, K.; Buchholz, C. J. Targeted Cell Entry of Lentiviral Vectors. *Mol. Ther.* **2008**, *16*, 1427–1436.
26. Cronin, J.; Zhang, X. Y.; Reiser, J. Altering the Tropism of Lentiviral Vectors through Pseudotyping. *Curr. Gene Ther.* **2005**, *5*, 387–398.
27. Lever, A.; Gottlinger, H.; Haseltine, W.; Sodroski, J. Identification of a Sequence Required for Efficient Packaging of Human Immunodeficiency Virus Type 1 RNA into Virions. *J. Virol.* **1989**, *63*, 4085–4087.
28. Hayashi, T.; Shioda, T.; Iwakura, Y.; Shibuta, H. RNA Packaging Signal of Human Immunodeficiency Virus Type 1. *Virology* **1992**, *188*, 590–599.
29. Zeffman, A.; Hassard, S.; Varani, G.; Lever, A. The Major HIV-1 Packaging Signal Is an Extended Bulged Stem Loop Whose Structure Is Altered on Interaction with the Gag Polyprotein. *J. Mol. Biol.* **2000**, *297*, 877–893.
30. Loo, L.; Guenther, R. H.; Basnayake, V. R.; Lommel, S. A.; Franzen, S. Controlled Encapsidation of Gold Nanoparticles by a Viral Protein Shell. *J. Am. Chem. Soc.* **2006**, *128*, 4502–4503.
31. Ishihama, Y.; Funatsu, T. Single Molecule Tracking of Quantum Dot-Labeled MRNAs in a Cell Nucleus. *Biochem. Biophys. Res. Commun.* **2009**, *381*, 33–38.
32. Yeh, H. Y.; Yates, M. V.; Mulchandani, A.; Chen, W. Molecular Beacon-Quantum Dot-Au Nanoparticle Hybrid Nanoprobes for Visualizing Virus Replication in Living Cells. *Chem. Commun.* **2010**, *46*, 3914–3916.
33. Zhou, P.; Zheng, Z.; Lu, W.; Zhang, F.; Zhang, Z.; Pang, D.; Hu, B.; He, Z.; Wang, H. Multicolor Labeling of Living-Virus Particles in Live Cells. *Angew. Chem., Int. Ed.* **2012**, *51*, 670–674.
34. Doan, L. X.; Li, M.; Chen, C.; Yao, Q. Virus-Like Particles as HIV-1 Vaccines. *Rev. Med. Virol.* **2005**, *15*, 75–88.
35. Cureton, D. K.; Massol, R. H.; Saffarian, S.; Kirchhausen, T. L.; Whelan, S. P. J. Vesicular Stomatitis Virus Enters Cells through Vesicles Incompletely Coated with Clathrin That Depend upon Actin for Internalization. *PLoS Pathog.* **2009**, *5*, e1000394.
36. Sun, X. J.; Yau, V. K.; Briggs, B. J.; Whittaker, G. R. Role of Clathrin-Mediated Endocytosis during Vesicular Stomatitis Virus Entry into Host Cells. *Virology* **2005**, *338*, 53–60.
37. Le Blanc, I.; Luyet, P. P.; Pons, V.; Ferguson, C.; Emans, N.; Petiot, A.; Mayran, N.; Demaurex, N.; Faure, J.; Sadoul, R.; *et al.* Endosome-to-Cytosol Transport of Viral Nucleocapsids. *Nat. Cell Biol.* **2005**, *7*, 653–664.
38. Brandenburg, B.; Zhuang, X. Virus Trafficking—Learning from Single-Virus Tracking. *Nat. Rev. Microbiol.* **2007**, *5*, 197–208.
39. Lakadamyali, M.; Rust, M. J.; Babcock, H. P.; Zhuang, X. Visualizing Infection of Individual Influenza Viruses. *Proc. Natl. Acad. Sci. U.S.A.* **2003**, *100*, 9280–9285.
40. Dohner, K.; Wolfstein, A.; Prank, U.; Echeverri, C.; Dujardin, D.; Vallee, R.; Sodeik, B. Function of Dynein and Dynactin in Herpes Simplex Virus Capsid Transport. *Mol. Biol. Cell* **2002**, *13*, 2795–2809.
41. McDonald, D.; Vodicka, M. A.; Lucero, G.; Svitkina, T. M.; Borisy, G. G.; Emerman, M.; Hope, T. J. Visualization of the Intracellular Behavior of HIV in Living Cells. *J. Cell Biol.* **2002**, *159*, 441–452.
42. Georgi, A.; Mottola-Hartshorn, C.; Warner, A.; Fields, B.; Chen, L. B. Detection of Individual Fluorescently Labeled Reovirions in Living Cells. *Proc. Natl. Acad. Sci. U.S.A.* **1990**, *87*, 6579–6583.
43. Li, F.; Chen, H.; Zhang, Y.; Chen, Z.; Zhang, Z. P.; Zhang, X. E.; Wang, Q. Three-Dimensional Gold Nanoparticle Clusters with Tunable Cores Templated by a Viral Protein Scaffold. *Small* **2012**, *8*, 3832–3838.
44. Wang, T.; Zhang, Z.; Gao, D.; Li, F.; Wei, H.; Liang, X.; Cui, Z.; Zhang, X. E. Encapsulation of Gold Nanoparticles by Simian Virus 40 Capsids. *Nanoscale* **2011**, *3*, 4275–4282.
45. You, J. O.; Liu, Y. S.; Liu, Y. C.; Joo, K. I.; Peng, C. A. Incorporation of Quantum Dots on Virus in Polycationic Solution. *Int. J. Nanomed.* **2006**, *1*, 59–64.
46. Gu, Y.; Yang, Y.; Liu, Y. Imaging Early Steps of Sindbis Virus Infection by Total Internal Reflection Fluorescence Microscopy. *Adv. Virol.* **2011**, *2011*, 535206.
47. Arhel, N. Revisiting HIV-1 Uncoating. *Retrovirology* **2010**, *7*, 96.
48. Miyauchi, K.; Kim, Y.; Latinovic, O.; Morozov, V.; Melikyan, G. B. HIV Enters Cells *via* Endocytosis and Dynamin-Dependent Fusion with Endosomes. *Cell* **2009**, *137*, 433–444.
49. Duan, H.; Nie, S. Cell-Penetrating Quantum Dots Based on Multivalent and Endosome-Disrupting Surface Coatings. *J. Am. Chem. Soc.* **2007**, *129*, 3333–3338.